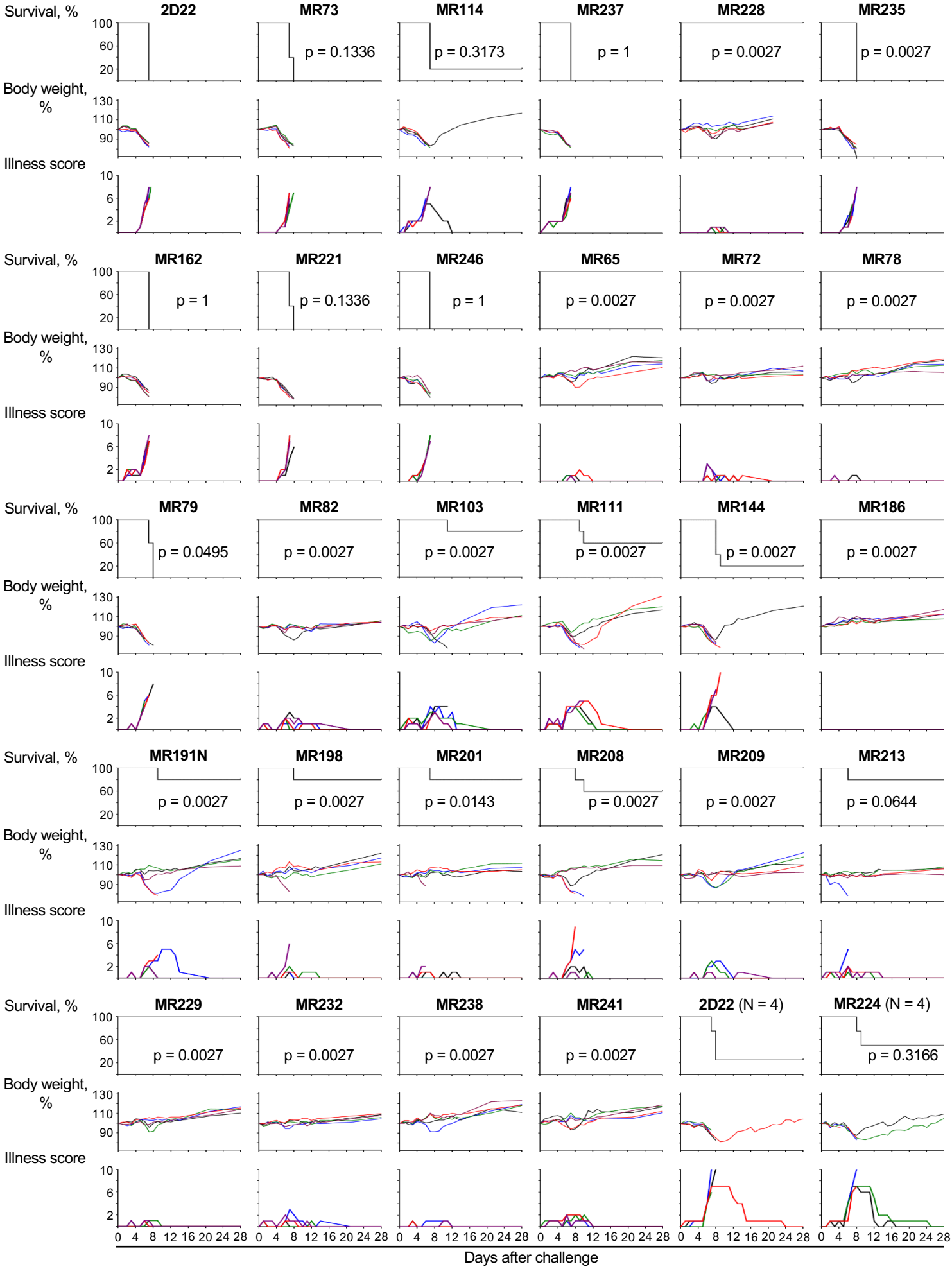

Suppl. Fig. 1 (related to Fig. 1). **Protective efficacy of human mAbs against lethal MARV challenge in mice** (see next page for the legend).

Suppl. Fig. 1 (related to Fig. 1)**. Protective efficacy of human mAbs against lethal MARV challenge in mice.** Groups of mice at five animals per group were injected with indicated mAbs by the IP route at 24 hours after MARV challenge. Kaplan-Meier survival curves, body weight and illness score curves are shown. Each group was compared to 2D22 control (Mantel-Cox test). The MR224 mAb was tested in comparison with 2D22 at four animals per group in a separate study.

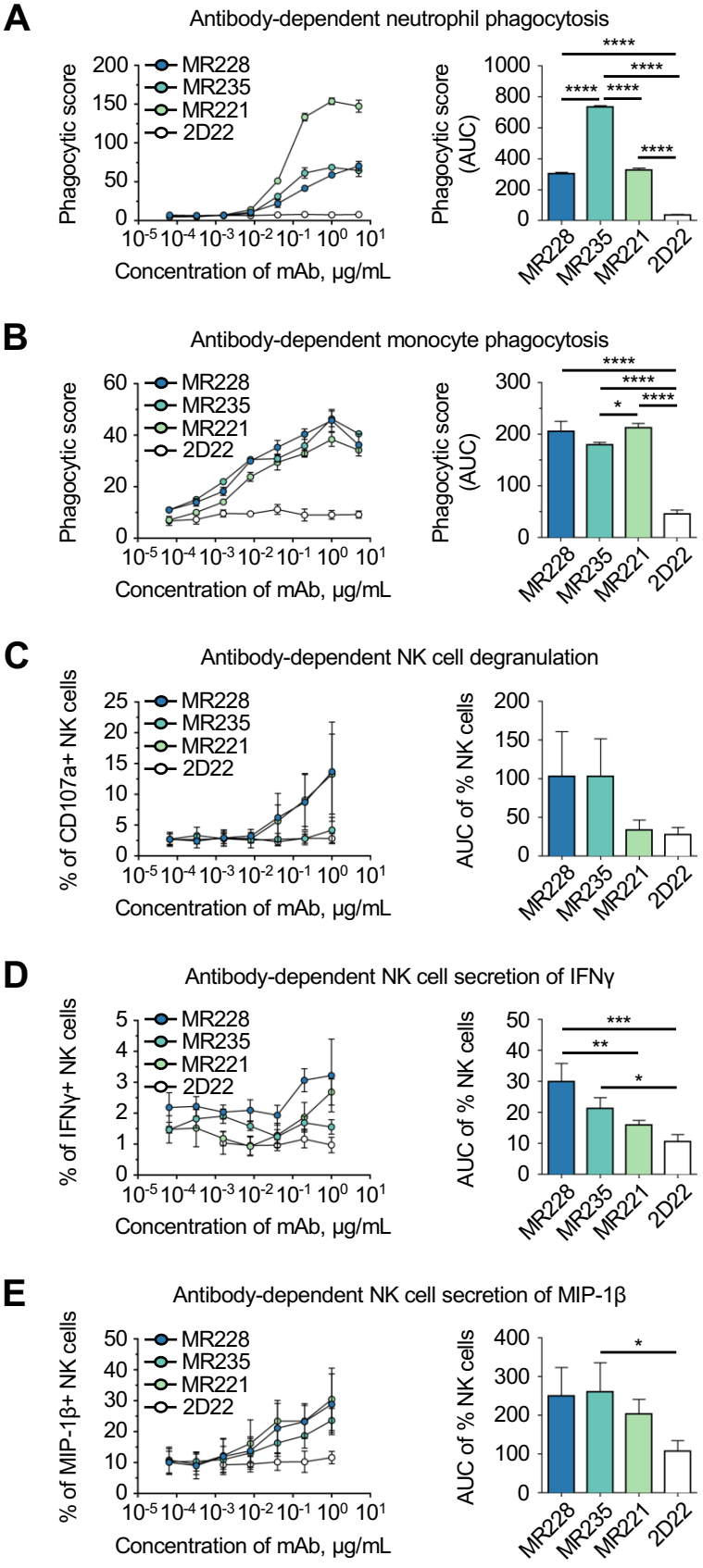

Suppl. Fig. 2 (related to Fig. 2A,B)**. Induction of innate immune effector functions by MR228 and MR235 mAbs.** Indicated mAbs were diluted in a 5-fold dilution curve and measured in triplicate for induction of **(A)** phagocytosis by primary human neutrophils; **(B)** phagocytosis by primary human monocytes; **(C)** degranulation of primary human NK cells; **(D)** secretion of IFNγ by primary human NK cells; and **(E)** secretion of MIP-1β by primary human NK cells. Considering that antibodies of IgG3 subclass have a higher affinity for the activating FcγRs over the other IgG subclasses (Bruhns et al., 2009), the IgG3 mAb from the panel, MR221, was used as a positive control in these experiments. The dilution curves are shown in the left graphs, and the area under the curve (AUC) for each mAb triplicate was calculated and is graphed in the right graphs. P values were calculated by One-Way ANOVA with Tukey's correction for multiple comparison testing: * p<0.05, ** p<0.01, *** p<0.001, **** p<0.0001.

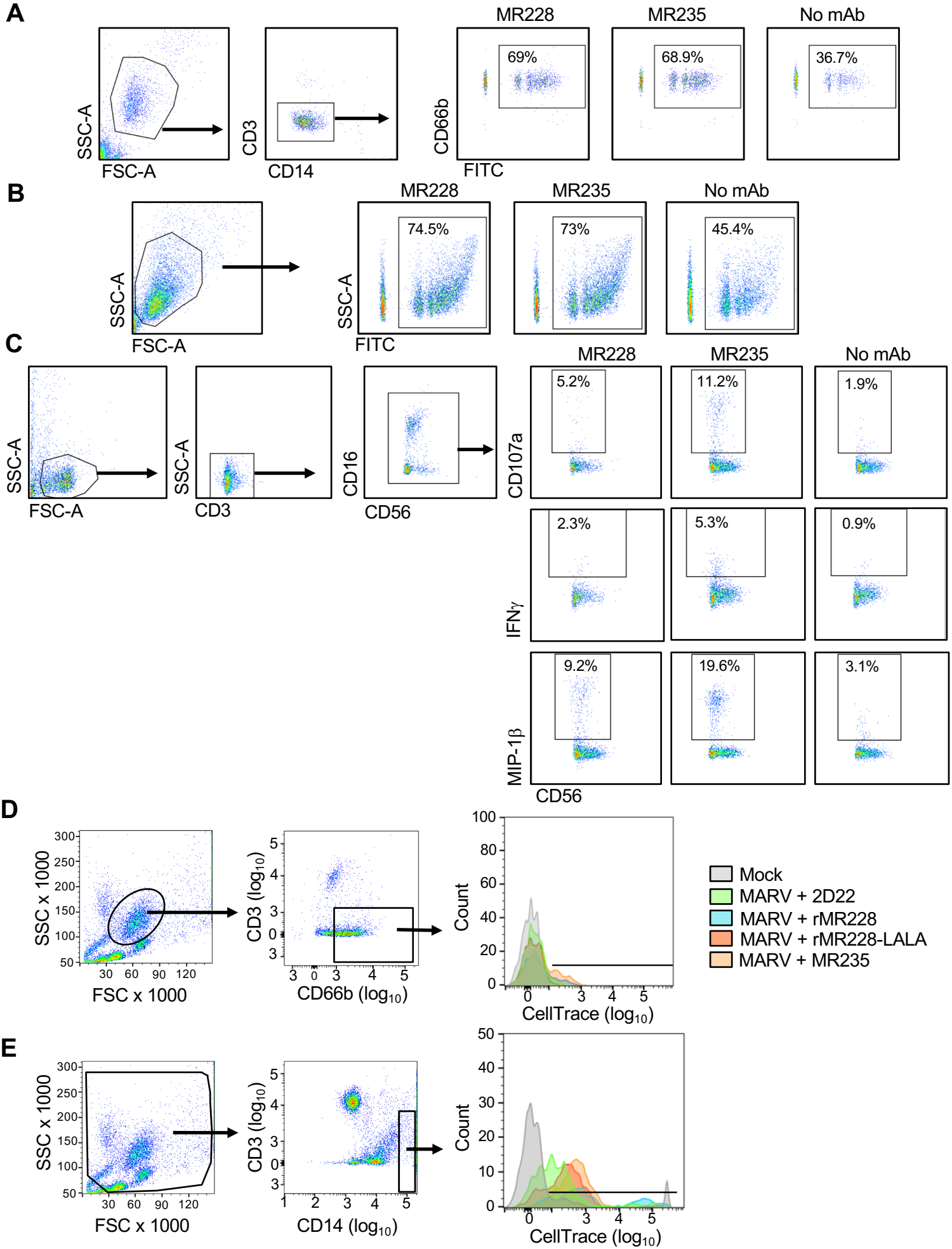

Suppl. Fig. 3 (related to Fig. 2). **Gating strategy for flow cytometric analysis of effector functions** (see next page for the legend).

Suppl. Fig. 3 (related to Fig. 2). **Gating strategy for flow cytometric analysis of effector functions. A-C**, representative flow cytometry plots for the indicated mAbs in response to stimulation with recombinant MARV GP: (A) ADNP, (B) ADCP, (C) antibody-dependent activation of NK cells. **D, E**, representative flow cytometry plots for the indicated mAbs in response to MARV infection: (D) ADNP, (E) ADCP. Neutrophils were defined as SSC-A^{high} CD66b^{+}, CD3^{-}, CD14^{-}, and monocytes were defined as CD3^{-} and CD14^{+}.

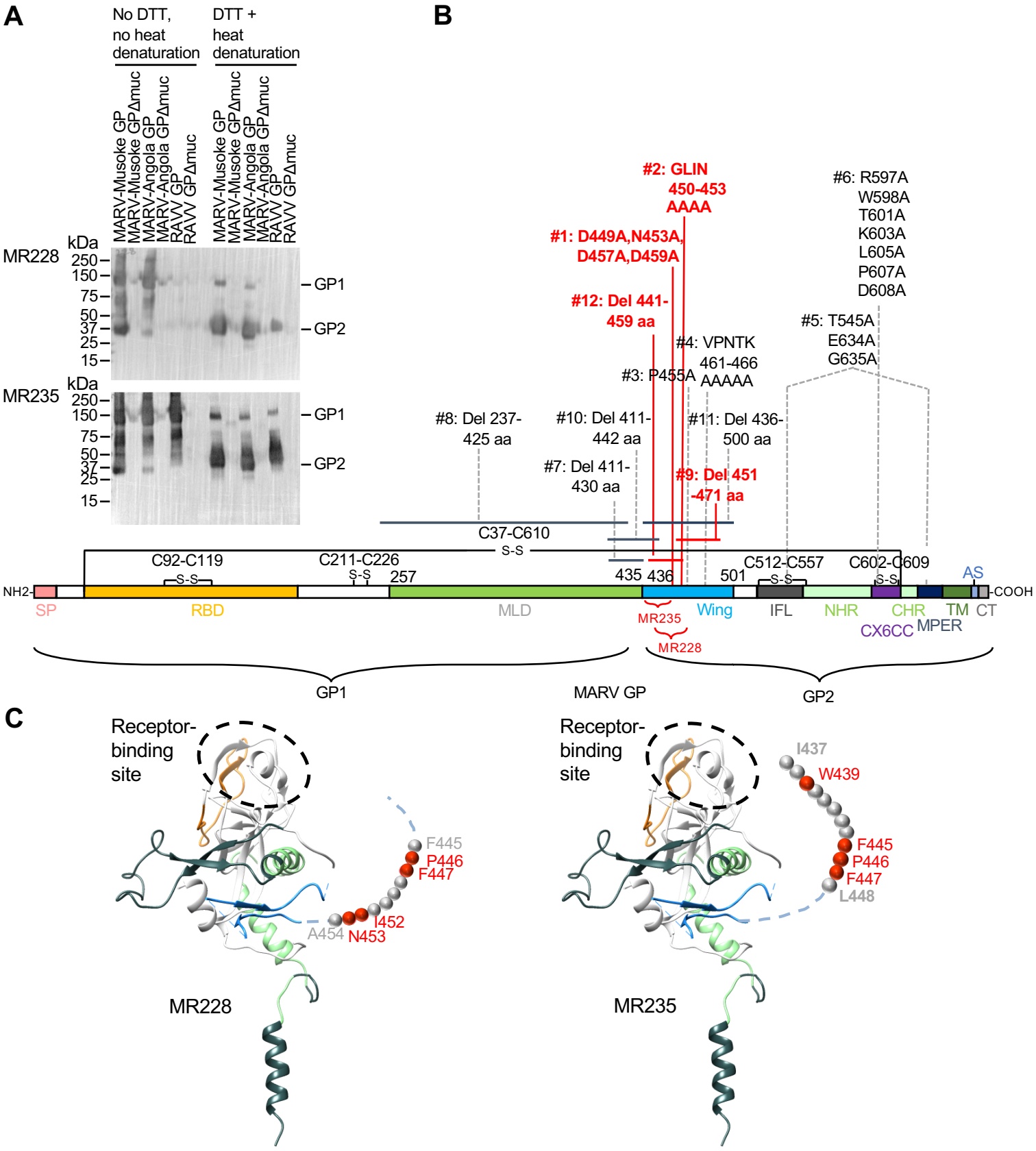

Suppl. Fig. 4 (related to Fig. 3)**. MR228 and MR235 bind linear epitopes in GP2 wing** (see next page for the legend)**.**

Suppl. Fig. 4 (related to Fig. 3)**. MR228 and MR235 bind linear epitopes in GP2 wing. (A)** Western blot analysis of binding of MR228 or MR235 to purified recombinant GPs of several MARV strains and RAVV under non-reducing (left) or reducing (right) conditions. DTT, dithiothreitol. **(B)** Epitope mapping of mAbs by flow cytometry analysis of their binding to GP constructs #1-12 with single or multiple mutations and/or deletions. MARV GP linear map (adapted from Mittler et al., 2013): SP, signal peptide (1-18 aa); RBD, receptor-binding domain (38-188 aa); MLD, mucin-like domain (257-501 aa); IFL, internal fusion loop (511-552 aa); NHR, N-terminal heptad repeat (553-596 aa); CX6CC, CX6CC motif (602-610 aa); CHR, C-terminal heptad repeat (616-633 aa); MPER, membrane-proximal external region (634-655 aa); TM, transmembrane anchor (659-667 aa); AS, acylation sites (aa 671 and 673); CT, cytoplasmic tail (674-681 aa). The red curly brackets indicate the binding sites for MR228 and MR235. Horizontal bars indicate constructs with corresponding deletions. Point mutations are indicated by vertical lines. The constructs which demonstrated a reduced binding of a specific mAb, but not of another mAb or reference polyclonal antibodies, are highlighted in red with positions of mutations indicated by red lines. Mutations in other constructs are indicated by dotted grey lines. Construct #6 designates a set of seven constructs with mutations in the aa 597-608 region (see Table S1). **(C)** Location of the epitopes on the GP structure. Epitope residues identified by mutagenesis (panel B) and peptide microarray (Fig. 3B,C) are shown in grey spheres and letters, and that identified by alanine scanning by red spheres and letters for each mAb are shown modeled with the MARV GP (PDB id 6BP2).

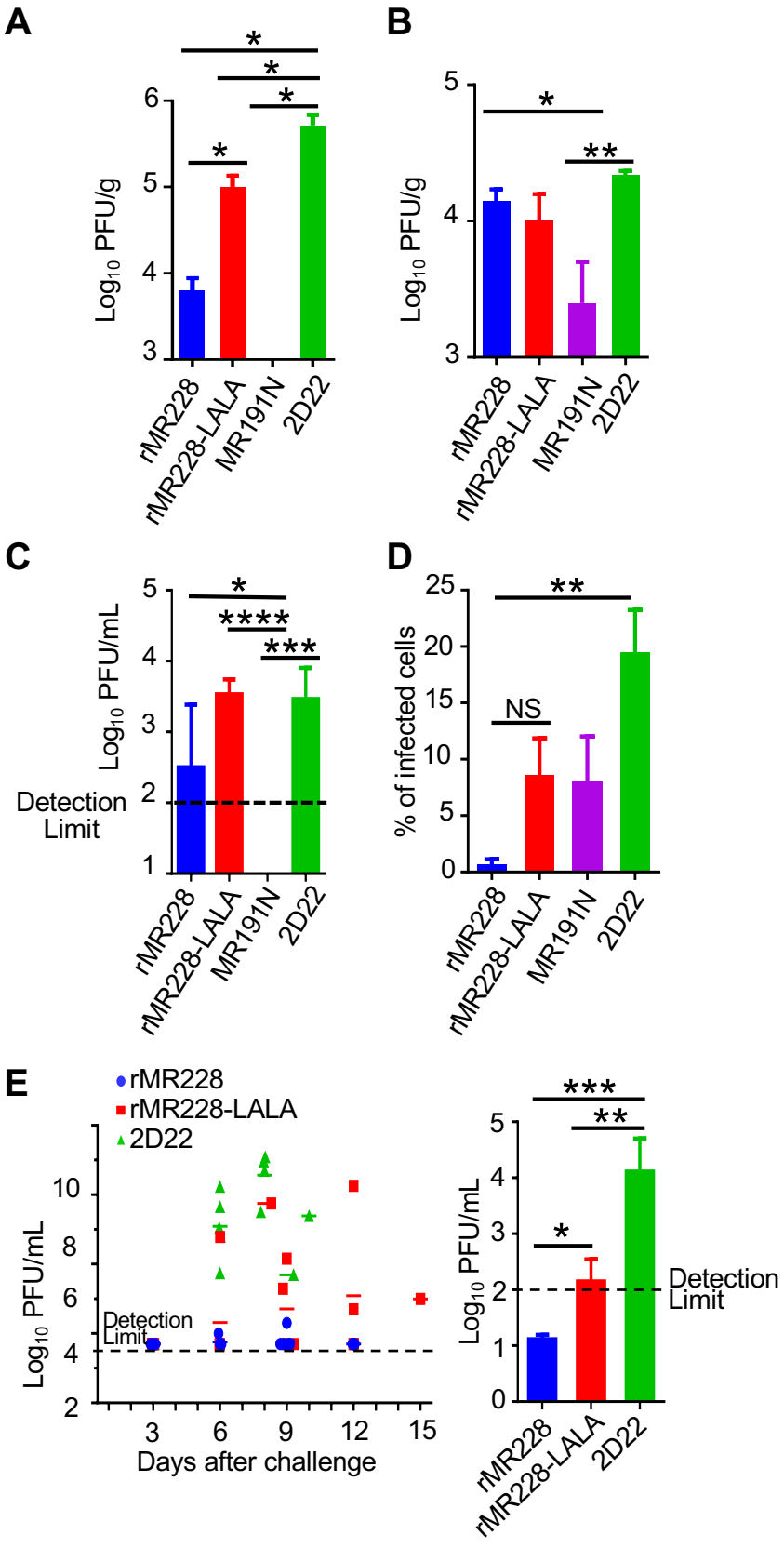

Suppl. Fig. 5 (related to Fig. 4)**. MR228 reduces virus load in blood and organs of infected animals. (A)** MARV titers in the spleen of mice on day 5 post infection. **(B)** MARV titers in the liver of mice on day 5 post infection. **(C)** MARV titers in the serum of mice on day 5 post infection. **(D)** Percentages of MARV-infected cells in the mesenteric lymph nodes of mice on day 5 post infection determined by flow cytometry. **(E)** MARV titers in the blood of infected guinea pigs. Left: titers for individual animals, right: within each group, viral titers (days 3 – 15 post infection) were pooled; for the samples in which no virus was detected, values 1 $\log_{10}$ below the detection limit were assigned for statistics analysis. Mean values ± SEM of replicates are shown. P values were calculated using unpaired Student's t-test: * $p < 0.05$, ** $p < 0.01$, *** $p < 0.001$, **** $p < 0.0001$, NS, not significant. A-D: 3 animals in 2D22 group and 4 animals in each of the other groups; E: 5 animals in each group.

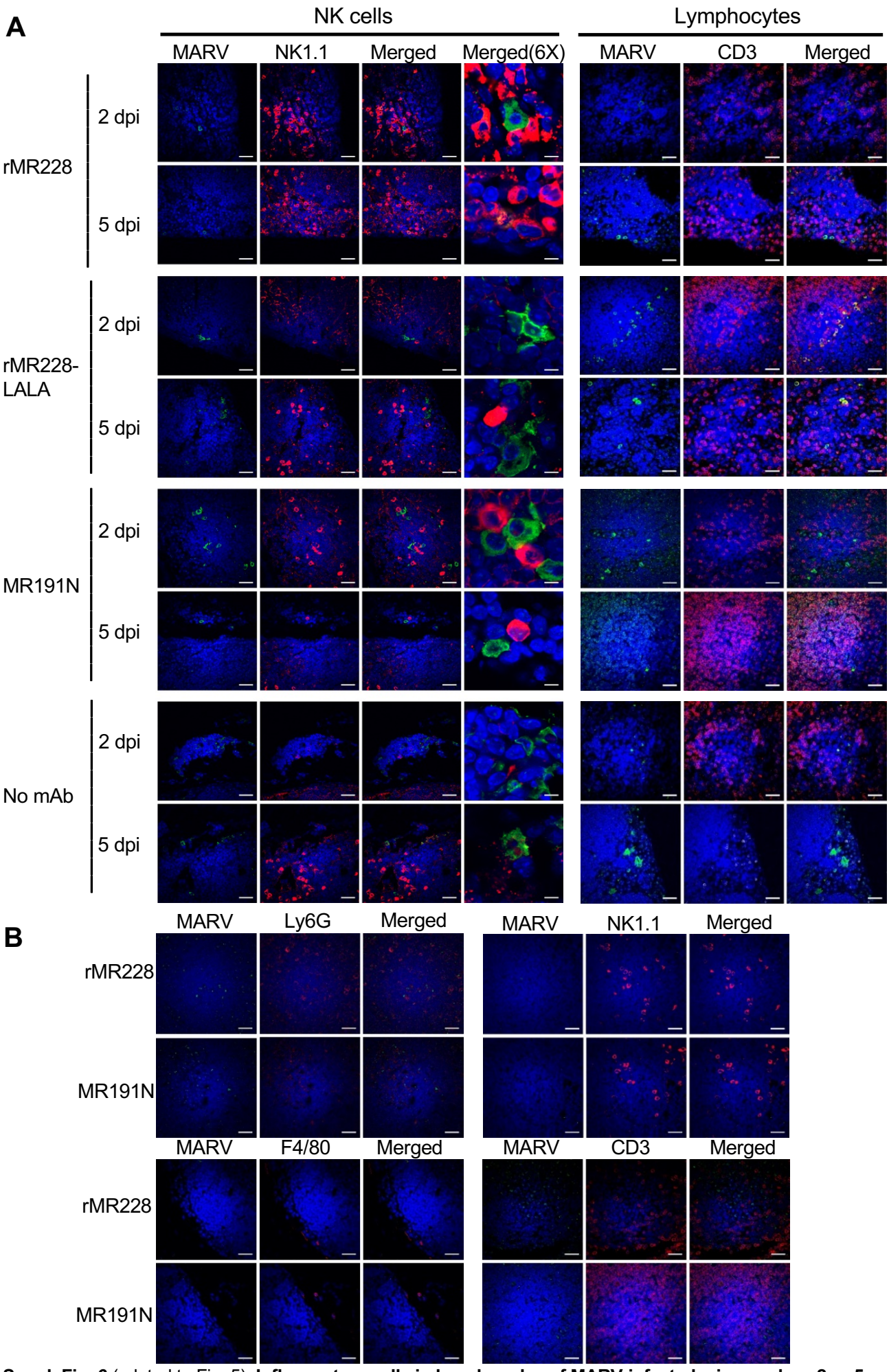

Suppl. Fig. 6 (related to Fig. 5). **Inflammatory cells in lymph nodes of MARV-infected mice on days 2 or 5 post infection** (see next page for the legend).

Suppl. Fig. 6 (related to Fig. 5)**. Inflammatory cells in lymph nodes of MARV-infected mice on days 2 or 5 post infection.** The scale bars correspond to 30 μm, or 5 μm for 6X zoom images. **(A)** Left panel, green, MARV; red, NK cells; right panel, green, MARV; red, lymphocytes. **(B)** Immune cells detected in lymph nodes of mock-infected mice. MARV was stained in green (not present). Red, the indicated immune cells. Neutrophils were stained for Ly6G, NK cells – for NK1.1, macrophages – for F4/80, and lymphocytes – for CD3.

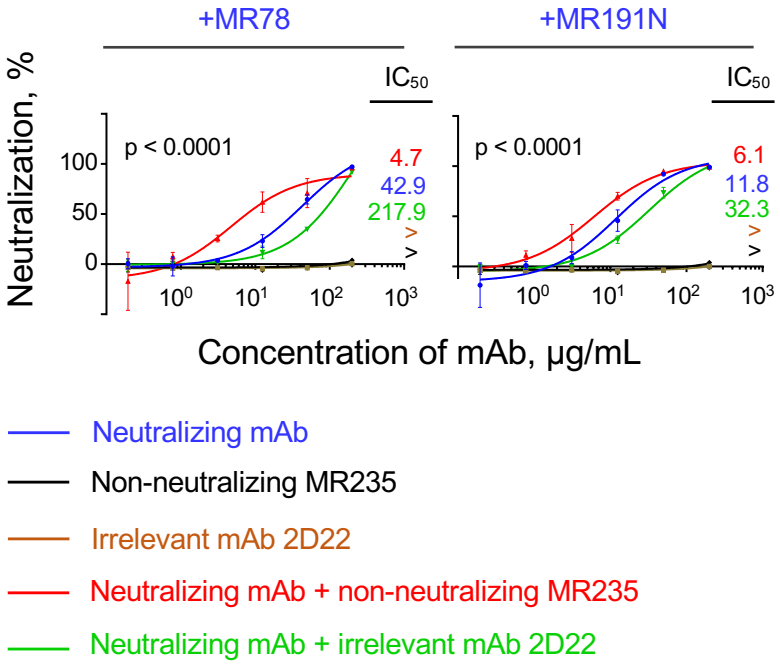

Suppl. Fig. 7 (related to Fig. 6)**. MR235 enhances mAb-mediated virus neutralization *in vitro*: a control experiment with the irrelevant mAb 2D22.** Percent neutralization by the indicated mAbs or their combinations. The values on the X axes indicate concentration of individual mAbs or 1:1 combinations of two mAbs. At any given concentration, the total amount of combined mAbs was the same as that of the individual mAbs. Mean ± SD of technical triplicates are shown. Mean IC_{50} values (µg/mL) for each mAb or combination are shown; > indicates neutralization was not detected at the highest concentration tested, 200 µg/mL. Each panel data were analyzed by One-Way ANOVA with Tukey's correction for multiple comparison testing; p values represent the comparison of IC_{50} (log_{10} µg/mL).

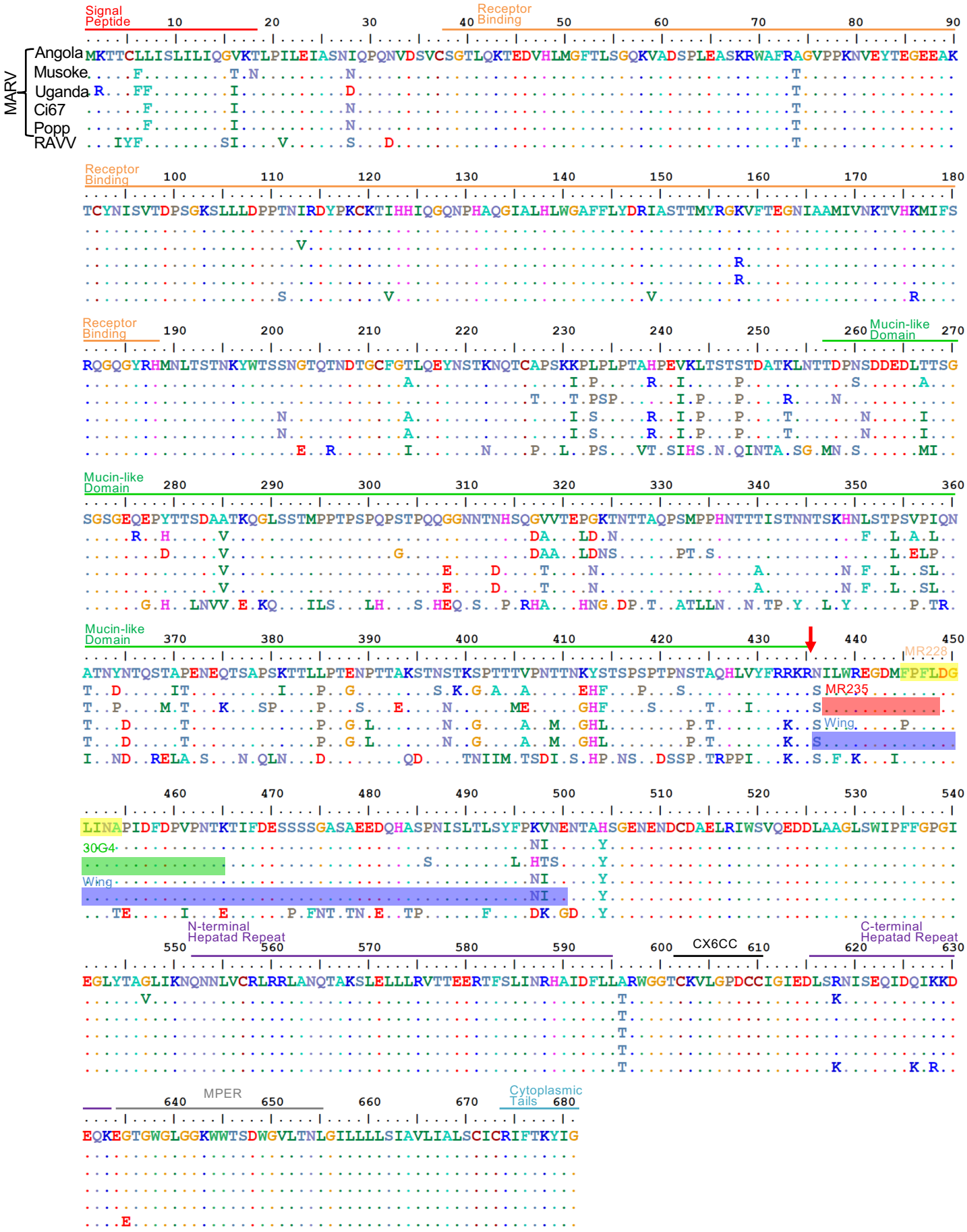

Suppl. Fig. 8 (related to Fig. 3)**. Conservation of various parts of GP.** Mucin-like domain is highly variable, whereas wing region is relatively conservative in GP among marburgviruses. Epitopes of three wing mAbs are highlighted in yellow (MR228), red (MR235) or green (30G4). Wing region is highlighted in blue. An arrow indicates the furin cleavage site.

Table S1 (related to Fig. 3A)**. Mutated MARV GP constructs generated for mapping of MR228 and MR235 epitopes.**

Mutant	Construction method	Enzymes used for GP cloning
450GLIN453 → AAAA	Site-directed mutagenesis	–
461VPNTK466 → AAAAA	Site-directed mutagenesis	–
D449A/N453A/D457A/D459A	Gene block synthesis	BstEII and PacI
T545A/E634A/G635A	Gene block synthesis	MfeI and NotI
P455A	Site-directed mutagenesis	–
R597A	Site-directed mutagenesis	–
W598A	Site-directed mutagenesis	–
T601A	Site-directed mutagenesis	–
K603A	Site-directed mutagenesis	–
L605A	Site-directed mutagenesis	–
P607A	Site-directed mutagenesis	–
D608A	Site-directed mutagenesis	–
Del 411-430aa	Gene block synthesis	BstEII and PacI
Del 237-425aa	Gene block synthesis	KpnI and PacI
Del 411-442aa	Gene block synthesis	BstEII and PacI
Del 436-500aa	Gene block synthesis	BstEII and PacI
Del 441-459aa	Gene block synthesis	BstEII and PacI